Electronic Supplementary Information

Effect of Incorporation of Gallium Ion into Silver Indium Sulfide Nanocrystals

Jiyeon Ban, [†a] *So Young Eom,* [†a] *Hak June Lee,*[bc] *Mai Ngoc An,*[d] *Beomsu Cho,*[a] *Yong Ho Lee,*[a] *Wan Ki Bae,*[b] *and Kwang Seob Jeong**[ad]

[a]Department of Chemistry, Korea University, Seoul 02841, Republic of Korea

[b]SKKU Advanced Institute of Nanotechnology (SAINT), Sungkyunkwan University (SKKU), Suwon 16419, Republic of Korea.

[c]School of Chemical and Biological Engineering, Seoul National University, Seoul 08826, Republic of Korea

[d]Center for Molecular Spectroscopy and Dynamics, Institute for Basic Science (IBS), Korea University, Seoul 02841, Republic of Korea

[Materials]

Gallium nitrate hydrate ($Ga(NO_3)_3 \cdot xH_2O$, Sigma-Aldrich, 99.9%), sodium diethyldithiocarbamate trihydrate (Na(DDTC), Sigma-Aldrich, ACS reagent), silver acetate (AgOAc, Sigma-Aldrich, 99%), indium acetate ($In(OAc)_3$, Sigma-Aldrich, 99.99%), zinc acetate ($Zn(OAc)_2$, Sigma-Aldrich, 99.99%), sulfur powder (Sigma-Aldrich, ≥99.5%), trioctylphosphine (TOP, Sigma-Aldrich, technical grade, 90%), oleylamine (OLAM, Sigma-Aldrich, technical grade, 70%), oleic acid (OA, DUKSAN), 1-octadecene (ODE, Sigma-Aldrich technical grade, 90%), 1-dodecanthiol (DDT, Sigma-Aldrich, ≥98%), chloroform (DAEJUNG), hexanes (DAEJUNG), methanol (DAEJUNG), molybdenum oxide (MoO_x, TASCO, 100 mesh powder, 99.995%), aluminum (TASCO, 5 mm × 5 mm Th pellets, Al, (TASCO, 99.999%), 4,4′-bis (carbazole-9-yl) biphenyl (CBP, OSM, 99.9%). Poly(3,4-ethylenedioxythiophene)-poly(styrenesulfonate) (PEDOT: PSS, Sigma-Aldrich, 1.3 wt. % dispersion in H_2O, conductive grade), poly(4-butyl-*N,N*-diphenylaniline) (Poly-TPD, Sigma-Aldrich, Mw ≥20,000 g/mol), zinc acetate dihydrate ($Zn(OAc)_2 \cdot 2H_2O$, Sigma-Aldrich, ACS reagent, ≥98%), potassium hydroxide (KOH, Sigma-Aldrich, 99.99%), chlorobenzene (Sigma-Aldrich, anhydrous, 99.8%), 2-propanol (IPA, DUKSAN, extra-pure). All chemicals were used without further purification.

[Procedures]

Preparation of gallium diethyldithiocarbamate ($Ga(DDTC)_3$)

Gallium diethyldithiocarbamate ($Ga(DDTC)_3$) was synthesized via a metathesis reaction between gallium nitrate $Ga(NO_3)_3$ and sodium diethyldithiocarbamate (Na(DDTC)). An aqueous solution of $Ga(NO_3)_3$ (50 mL, 0.1 M) was mixed with an aqueous solution of Na(DDTC) (50 mL, 0.1 M). The reaction mixture was then stirred under ambient conditions for 2 h. Upon completion of the reaction, the mixture was filtered through a vacuum filter to obtain the product, which was dried overnight under vacuum.

Synthesis of AIGS core nanocrystals

AIGS core nanocrystals (NCs) were synthesized using a heat-up method. A three-neck round-bottom flask (RBF) containing AgOAc (0.1 mmol), $In(OAc)_3$ (0.05 mmol), $Ga(DDTC)_3$ (0.15 mmol), OLAM (3 mL), OA (2 mL), and ODE (2 mL) was degassed for approximately 1–2 h at 100 °C under vacuum. After degassing, the temperature of the flask was raised to the desired synthesis temperature (150–280 °C) under an argon atmosphere. After 30 min, the reactor was quenched using an air blower and ice bath. The crude solution was centrifuged at 3000 rpm for 2 min to remove any residual byproducts. Subsequently, the NCs were precipitated and purified by adding an appropriate volume of a chloroform/methanol mixture, followed by centrifugation at 3000 rpm for 5 min. Finally, the obtained AIGS NCs were redispersed in hexane for further measurements and synthesis.

Synthesis of AIGS/ZnS core-shell nanocrystals

AIGS/ZnS core-shell NCs were synthesized using the successive ionic layer adsorption and reaction (SILAR) method. A RBF containing pre-synthesized AIGS NCs (0.6 mL, 40 mg/mL), OLAM (3 mL), OA (1 mL), DDT (1 mL), and ODE (3 mL) was degassed for 1–2 h at 80 °C. After

degassing, the temperature was raised under an argon atmosphere to 140 °C, after which the ZnS precursor (2 mL, 0.2 M; obtained by dissolving $Zn(OAc)_2$ and sulfur powder in TOP) was injected dropwise. After 20 min, another aliquot of the ZnS precursor solution was injected into the mixture, and the reaction was allowed to proceed for 1 h. The purification process for these NCs was identical to that for the AIGS core NCs. Purified NCs were redispersed in hexane for further analysis.

Fabrication of electroluminescence device

The following procedure was used to fabricate the electroluminescence (EL) device (ITO/ZnO or $Zn_{0.9}MgO$ (30 nm)/NCs/CBP (60 nm)/MoOx (10 nm)/Al (120 nm)): ZnO nanoparticles (20 mg/mL) were spun-cast on the ITO substrate at 2000 rpm for 30 sec and annealed for 30 min at 75 °C on a hotplate, which was placed in a glovebox. AIGS/ZnS core/shell NCs (7 mg/mL) were spin-cast at 4000 rpm for 30 s on ZnO/ITO and annealed at 75 °C for 30 min in a glovebox. CBP (60 nm), MoO_x (10 nm), and Al (110 nm) were thermally evaporated on the NCs/ZnO/ITO films under 10^{-6} torr at deposition rates of 1.0–1.5, 0.1–0.2, and 1.0–2.0 Å/s respectively.

For the fabrication of the normal EL device (ITO/ PEDOT:PSS/Poly-TPD/ NCs/ ZnO/Al), PEDOT:PSS were spun-cast on the ITO substrate at 4000 rpm for 1 min and annealed at 150 °C for 45 min on a hotplate, which was placed in a glovebox. A Poly-TPD layer was spun-cast at 2500 rpm for 45 sec on the PEDOT:PSS film, followed by annealing at 50 °C for 20 min. ZnO NCs (45 mg/mL of ZnO NCs) were spin-cast at 3000 rpm for 1 min and annealed at 120 °C for 30 min in a glove box. Al (80 nm) was thermally deposited at 10^{-6} torr at a deposition rate of 1.2 Å/s.

After fabrication, the device was encapsulated in glass and sealed with UV resin.

[Characterization methods]

X-ray Diffraction measurement

A D8 Discover (Bruker AXS GmbH) X-ray diffractometer with graphite-monochromatized Cu anode material and a 6 kW high power was used for the structural analysis. The spectra were collected at 20 to 60 degrees with an increase of 0.01°.

Transmission electron microscopy

A Tecnai 20 instrument with an acceleration voltage of 200 kV and LaB6 as the electron source was used to measure the size of the NCs. The size, morphology, and elemental composition of the NCs were determined using a JEOL JEM-F200 instrument. The accelerating voltage was 200 kV and the resolution was 0.23 nm.

Photoluminescence spectroscopy

The photoluminescence measurements were performed using a Hitachi F-7000 fluorescence spectrometer (Hitachi Ltd., Japan). Photoluminescence (PL) spectra were collected using emission slit widths of 5 nm, a PMT voltage of 400 V, and scan speed of 240 nm/min. The excitation wavelength was 371 nm. The absolute photoluminescence quantum yield (PLQY) of the NCs solutions was measured using an FP-8500 spectrofluorometer (JASCO) equipped with an integrating sphere (ILF-835). The excitation wavelength was 371 nm, and the NCs solution was diluted to 1.0 at the excitation wavelength (371 nm).

Time-resolved photoluminescence measurement

Fluorolog3 with time-correlated single-photon counting (TCSPC) (HORIBA SCIENTIFIC) was used to measure the PL lifetimes of the NCs. Time-resolved photoluminescence (TR-PL) was measured in the liquid phase. The spectra were then fitted to three components. The exponential decay was fitted using the following equation:

$$I(t) = A_1 e^{-\frac{t}{\tau_1}} + A_2 e^{-\frac{t}{\tau_2}} + A_3 e^{-\frac{t}{\tau_3}}, \quad (1)$$

where $I(t)$ is the spectral intensity, A_n is the amplitude of each component, τ_n is the decay time.

The average decay time (τ_{avg}) was calculated using following equations:

$$1 = A_1 + A_2 + A_3, \quad (2)$$

$$\tau_{avg} = A_1 \times \tau_1 + A_2 \times \tau_2 + A_3 \times \tau_3, \quad (3)$$

X-ray photoelectron spectroscopy and ultraviolet photoelectron spectroscopy

A Thermo Scientific Nexsa instrument with a monochromated, micro-focused, low-power Al Ka X-ray source was used to measure the XPS and ultraviolet photoelectron spectroscopy (UPS) spectra. Each sample was prepared using a spin-coated film deposited on a Si substrate. The valence band maximum was calculated using the following equation:

$$VBM = h\upsilon - (E_{onset} - E_{cutoff}), \quad (4)$$

where $h\upsilon$ is the He(I) source energy (21.22 eV).

Device measurement

The current-voltage curve of the EL device was obtained using a Keithley-236 source-measure unit, a Keithley multimeter unit coupled with a calibrated Si photodiode (Hamamatsu S5227-1010BQ), and a photomultiplier tube detector. EL spectra were measured using a spectroradiometer (Konica Minolta CS-2000).

Table S1. Atomic ratio calculated by energy dispersive spectroscopy mapping.

°C	Ag (%)	In (%)	Ga (%)	S (%)
150	25.54	17.80	21.53	35.14
210	26.31	9.70	22.97	41.02
280	23.16	9.43	23.49	43.92

Table S2. Fitting information of PL of (a) AIGS-150 (b) AIGS-180 (c) AIGS-210 (d) AIGS- 250 (e) AIGS-280

(a)

Fit function	Gaussian function	
PL maximum (nm)	633.52 ± 0.07	706.66 ± 0.19
Coefficient of determination	0.99978	

(b)

Fit function	Gaussian function		
PL maximum (nm)	547.65 ± 0.08	630.99 ± 0.04	711.88 ± 0.17
Coefficient of Determination	0.99987		

(c)

Fit function	Gaussian function	
PL maximum (nm)	547.82 ± 0.05	601.24 ± 0.49
Coefficient of determination	0.99774	

(d)

Fit function	Gaussian function	
PL maximum (nm)	556.10 ± 0.04	599.35 ± 0.38
Coefficient of determination	0.99789	

(e)

Fit function	Gaussian function
PL maximum (nm)	549.97 ± 0.04
Coefficient of determination	0.99726

Table S3. Fitting information of Ga3d XPS of (a) AIGS-150, (b) AIGS-180, (c) AIGS-210, (d) AIGS- 250, (e) AIGS-280

(a)

Fit function	Gaussian function		
Plot	Peak1	Peak2	Peak3
y_0	313.09 ± 68.34	313.09 ± 68.34	313.09 ± 68.34
x_c	17.99± 0.02	18.88 ± 0.03	19.83 ± 0.06
A	28326.97 ± 1039.72	4065.62 ± 1359.98	9338.15 ± 862.84
w	1.43 ± 0.03	0.83 ± 0.09	1.49 ± 0.10
R-Square (COD)	0.99878		

(b)

Fit function	Gaussian function		
Plot	Peak1	Peak2	Peak3
y_0	87.69 ± 40.87	87.69 ± 40.87	87.69 ± 40.87
x_c	18.00± 0.03	18.90 ± 0.04	19.92 ± 0.04
A	8671.89 ± 513.56	1588.41 ± 650.36	6077.86 ± 411.26
w	1.36 ± 0.06	0.81 ± 0.12	1.51 ± 0.08
R-Square (COD)	0.99611		

(c)

Fit function	Gaussian function		
Plot	Peak1	Peak2	Peak3
y_0	37.85 ± 29.59	37.85 ± 29.59	37.85 ± 29.59
x_c	17.94 ± 0.04	18.74 ± 0.03	19.87 ± 0.01
A	4372.58 ± 289.53	693.08 ± 247.73	10523.42 ± 141.45
w	1.33 ± 0.07	0.62 ± 0.10	1.41 ± 0.02
R-Square (COD)	0.99793		

(d)

Fit function	Gaussian function		
Plot	Peak1	Peak2	Peak3
y_0	152.90 ± 28.21	152.90 ± 28.21	152.90 ± 28.21
x_c	17.86 ± 0.06	18.68 ± 0.04	19.78 ± 0.01
A	4470.42 ± 362.31	553.20 ± 272.99	7659.23 ± 145.41
w	1.54 ± 0.10	0.64 ± 0.14	1.32 ± 0.02
R-Square (COD)	0.99609		

(e)

Fit function	Gaussian function		
Plot	Peak1	Peak2	Peak3
y_0	-16.34 ± 31.62	-16.34 ± 31.62	-16.34 ± 31.62
x_c	18.04 ± 0.03	18.81 ± 0.03	19.93 ± 0.01
A	5623.54 ± 299.97	429.71 ± 188.74	12830.71 ± 143.73
w	1.47 ± 0.06	0.54 ± 0.12	1.38 ± 0.01
R-Square (COD)	0.99847		

Table S4. Fitted parameter of time-resolved photoluminescence (TR-PL) spectra of AIGS NCs

	A1	$\tau_{1(ns)}$	A2	$\tau_{2(ns)}$	A3	$\tau_{3(ns)}$	y0	Average decay time (ns)
AIGS-150 Em@636 nm	0.32	66	0.52	331	0.16	850	88.03	329
AIGS-250 Em@558 nm	0.38	102	0.04	595	0.58	23	18.00	74
AIGS-250 Em@612 nm	0.37	279	0.07	1080	0.56	439	54.52	204
AIGS-280 Em@555 nm	0.36	103	0.03	604	0.61	23	16.19	71

Table S5. Fitted parameter and Average decay time Measured by Time-Resolved Photoluminescence of AIGS NCs

	A_1	$\tau_{1(s)}$	A_2	$\tau_{2(s)}$	A_3	$\tau_{3(s)}$	y_0	average decay time (s)
AIGS-150 Em@551 nm	39.98 %	1.45×10^{-7}	14.23 %	4.94×10^{-7}	45.79 %	2.06×10^{-8}	49.81	1.38×10^{-7}
AIGS-150 Em@636 nm	32.40 %	6.75×10^{-8}	51.51 %	3.31×10^{-7}	16.08 %	8.05×10^{-7}	88.03	3.29×10^{-7}
AIGS-180 Em@551 nm	36.58 %	2.89×10^{-7}	8.78 %	1.30×10^{-6}	54.64 %	4.62×10^{-8}	121.75	2.45×10^{-7}
AIGS-180 Em@636 nm	56.12 %	5.81×10^{-7}	10.84 %	1.73×10^{-6}	33.04 %	1.30×10^{-7}	190.12	5.57×10^{-7}
AIGS-210 Em@560 nm	31.69 %	3.58×10^{-7}	5.55 %	1.67×10^{-6}	62.76 %	6.08×10^{-8}	76.96	2.44×10^{-7}
AIGS-210 Em@616 nm	48.42 %	5.67×10^{-7}	8.79 %	1.95×10^{-6}	42.79 %	1.30×10^{-7}	141.66	5.02×10^{-7}
AIGS-250 Em@558 nm	37.83 %	1.02×10^{-7}	3.62 %	5.95×10^{-7}	58.55 %	2.26×10^{-8}	18.00	7.35×10^{-8}
AIGS-250 Em@612 nm	37.12 %	2.79×10^{-7}	7.01 %	1.08×10^{-6}	55.79 %	4.39×10^{-8}	54.52	2.04×10^{-7}
AIGS-280 Em@555 nm	36.04 %	1.03×10^{-7}	3.34 %	6.04×10^{-7}	60.62 %	2.28×10^{-8}	16.18	7.12×10^{-8}

Table S6. (a) The lattice parameter of AIGS core NCs and shell materials utilized in the core/shell synthesis, (b) calculated lattice mismatch with hexagonal Ga_2S_3, and (c) zinc blende ZnS.

(a)

	tetragonal AIGS	**tetragonal AGS**	**tetragonal AIS**	**Zinc blende ZnS**	**Hexagonal Ga_2S_3**
a	5.83 Å	5.76 Å	5.93 Å	5.41 Å	3.50 Å
c	10.43 Å	10.30 Å	11.52 Å		15.49 Å

(b)

	a	**c**
$AgIn_xGa_{1-x}S_2$	7.14 %	86.11 %
$AgGaS_2$	6.42 %	83.99 %
$AgInS_2$	9.61 %	104.87 %

Table S7. Calculated Atomic Ratio by EDS analysis

Ag	In	Ga	S	Zn
21.16 %	8.57 %	17.23 %	42.11 %	10.93 %

Figure S1. EDS mapping image of AIGS NCs synthesized at (a) 150°C, (b) 210°C, (c) 280°C, and (d) calculated atomic ratio by X-ray Photoelectron Spectroscopy.

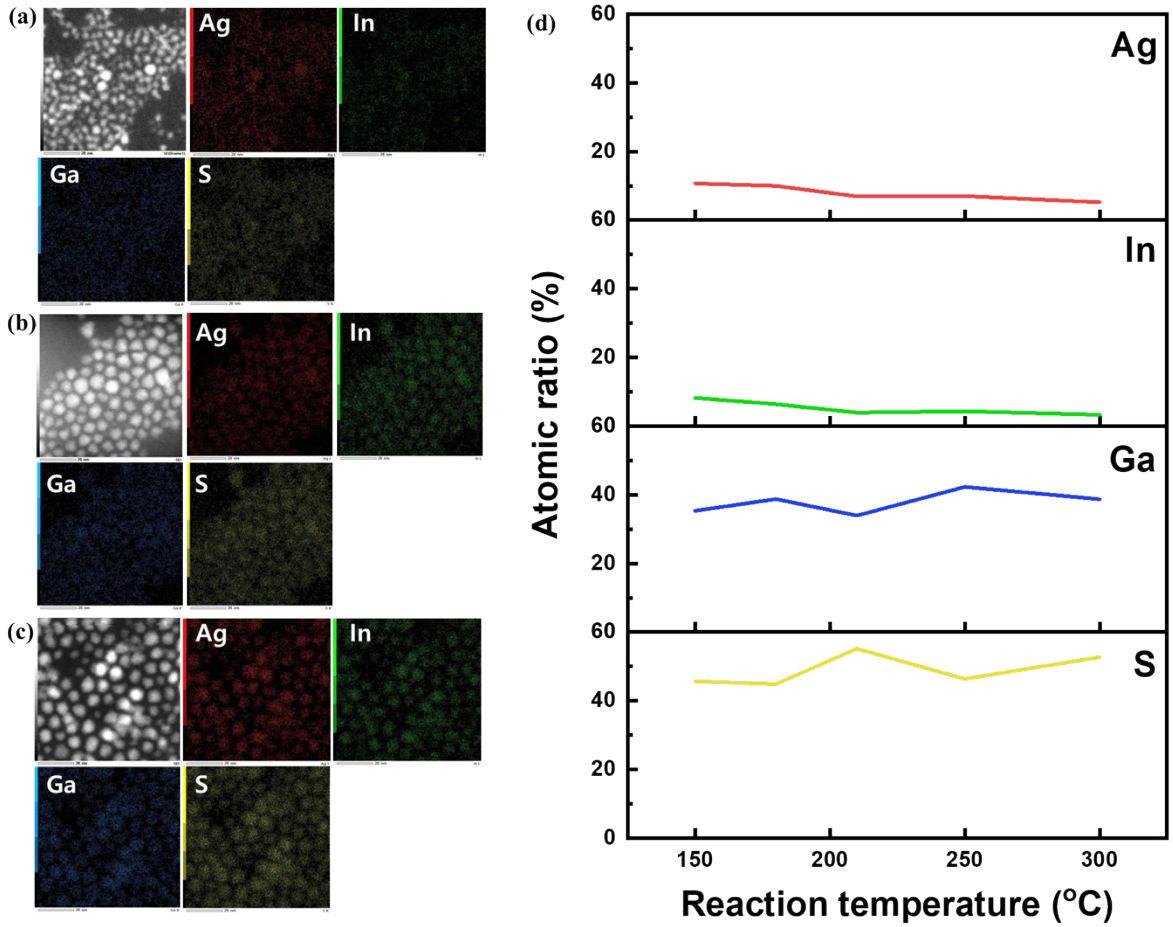

Figure S2. (a) Absorption and photoluminescence and (b)XPS spectrum of AIGS NCs which shows the minimum full-width half maximum (FWHM)

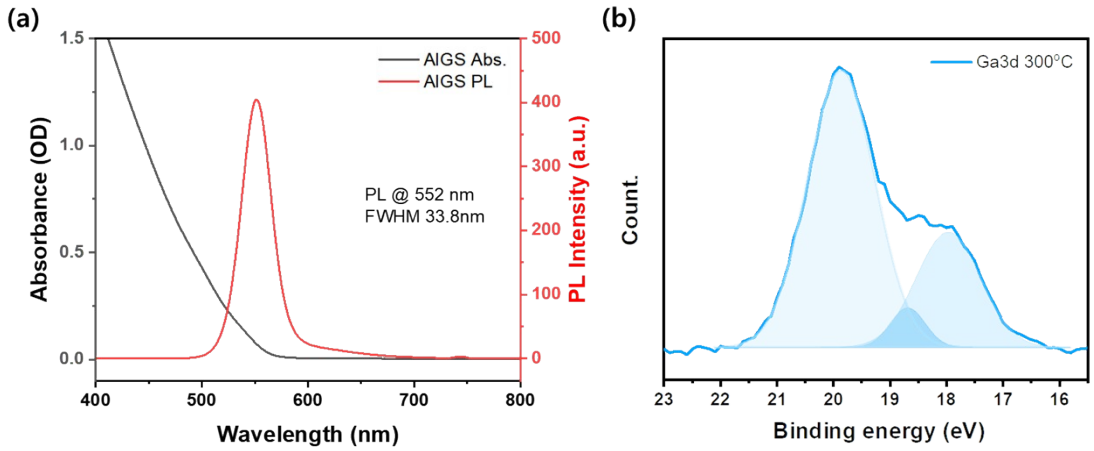

Figure S3. XPS spectra of (a) Ag3d, (b) In 3d, (c) S2p of AIGS NCs synthesized at each temperature.

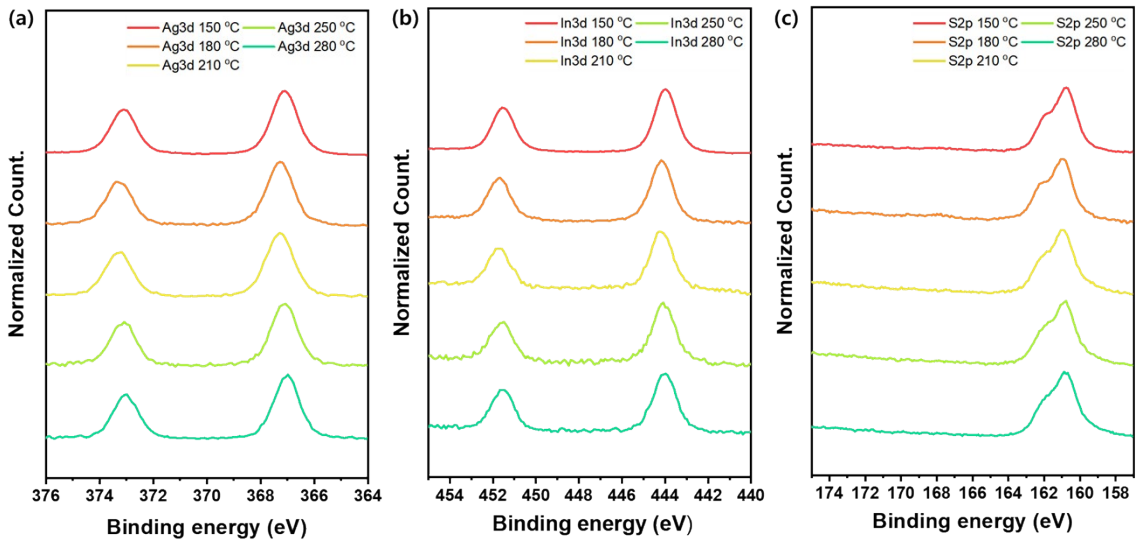

Figure S4. time-resolved photoluminescence (TR-PL) spectra of AIGS NCs synthesized at each temperature.

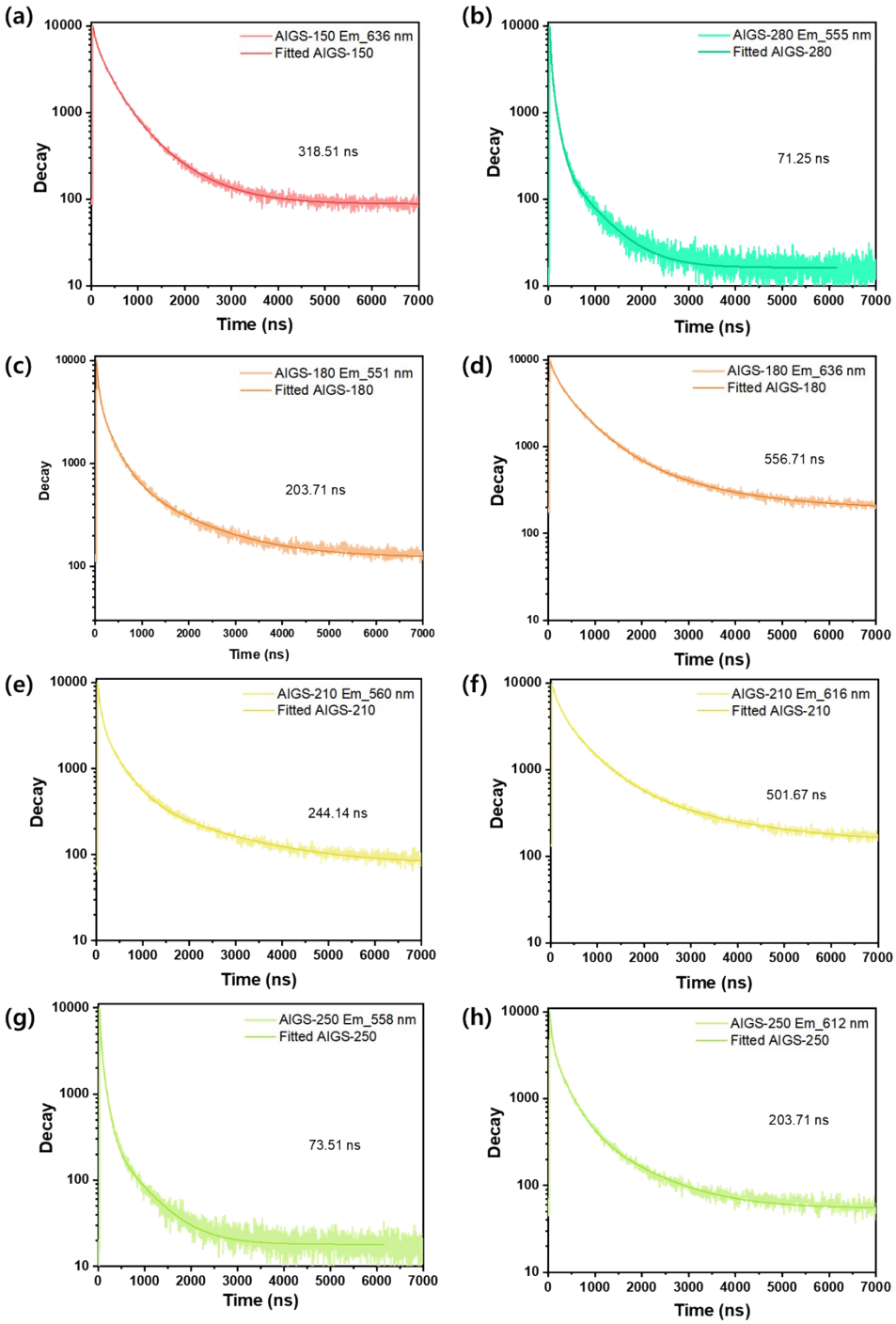

Figure S5. (a) the ^{1}H-NMR spectrum of OA, (b) the ^{1}H-NMR spectrum of OLAM, (c) the ^{1}H-NMR spectrum of the mixture of OA and OLAM (molar ratio, 1:1), which is consistent with that of OA-OLAM, and (d) the ^{1}H-NMR spectrum of the AIGS NCs showing OOA as the major component in $CDCl_3$.[1]

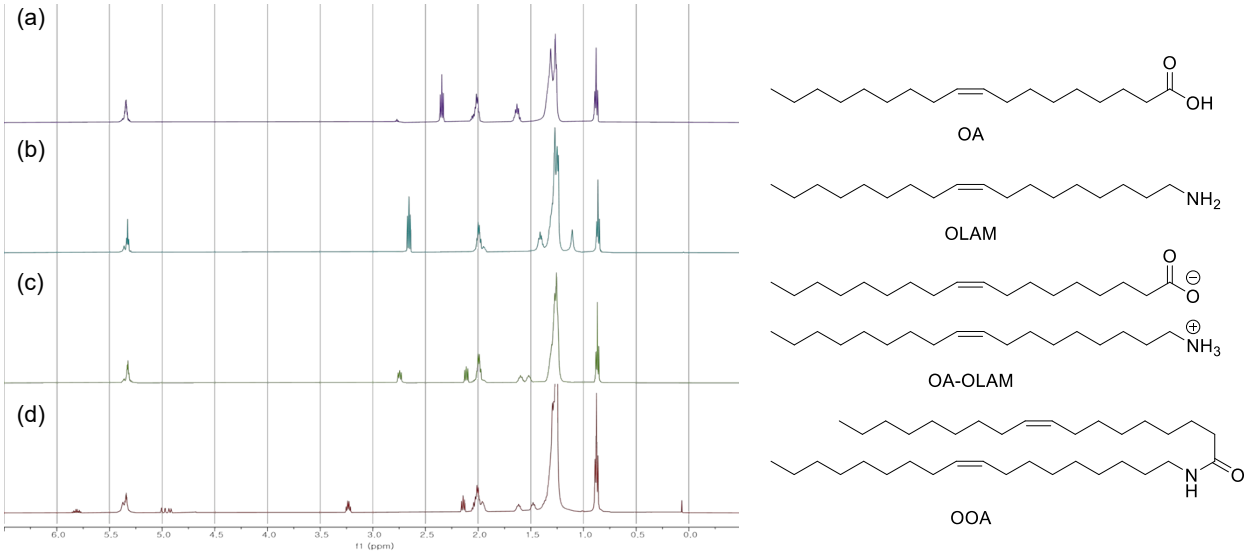

Figure S6. EDS Mapping Image of AIGS/ZnS NCs

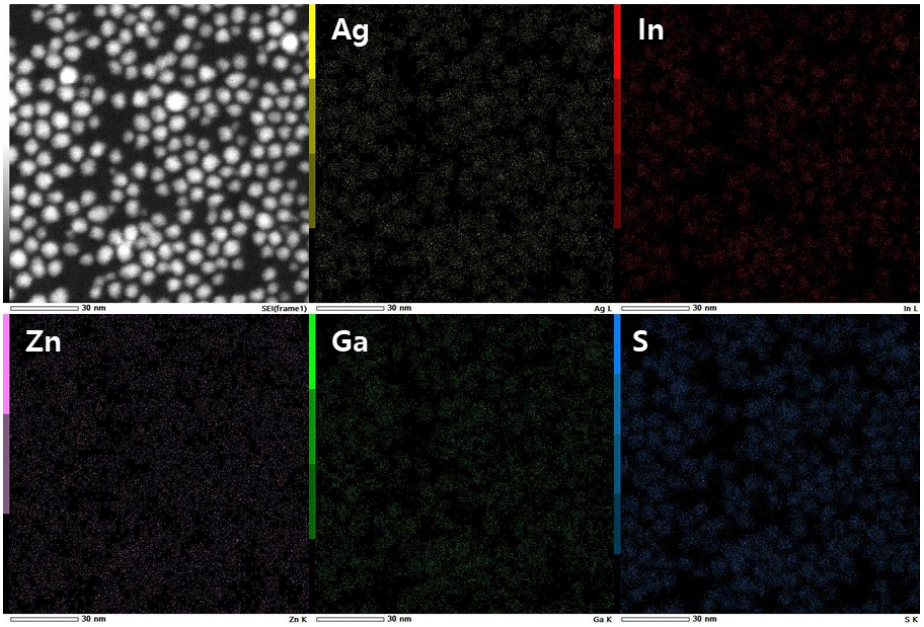

Figure S7. (a) PL spectra of AIGS core NCs, (b) AIGS/ZnS NCs-1; injection 2mL of ZnS precursor to core NCs followed by 20 min of reaction time, and (c) AIGS NCs-2; injection 2mL of ZnS precursor to AIGS/ZnS-1 followed by 1hr of reaction time

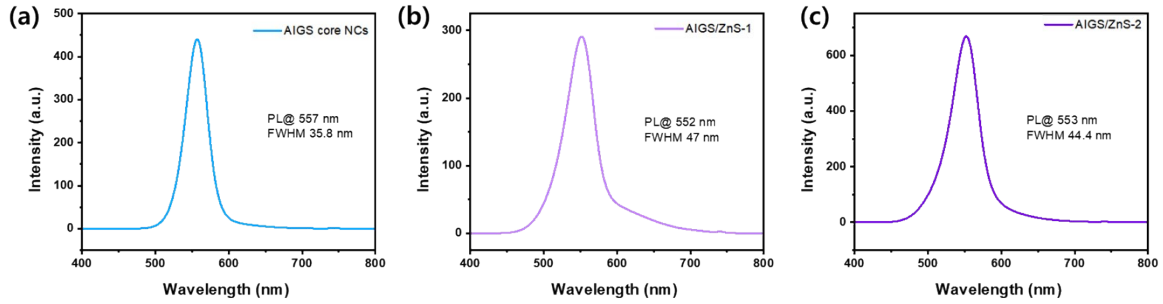

Figure S8. (a) Device structure, (b) Energy level of each layer, (c) J-V curve, (d) Electroluminescence spectra, (e) Luminance efficiency and external quantum efficiency (EQE), and (f) Emitting photograph of AIGS/ZnS-based EL device

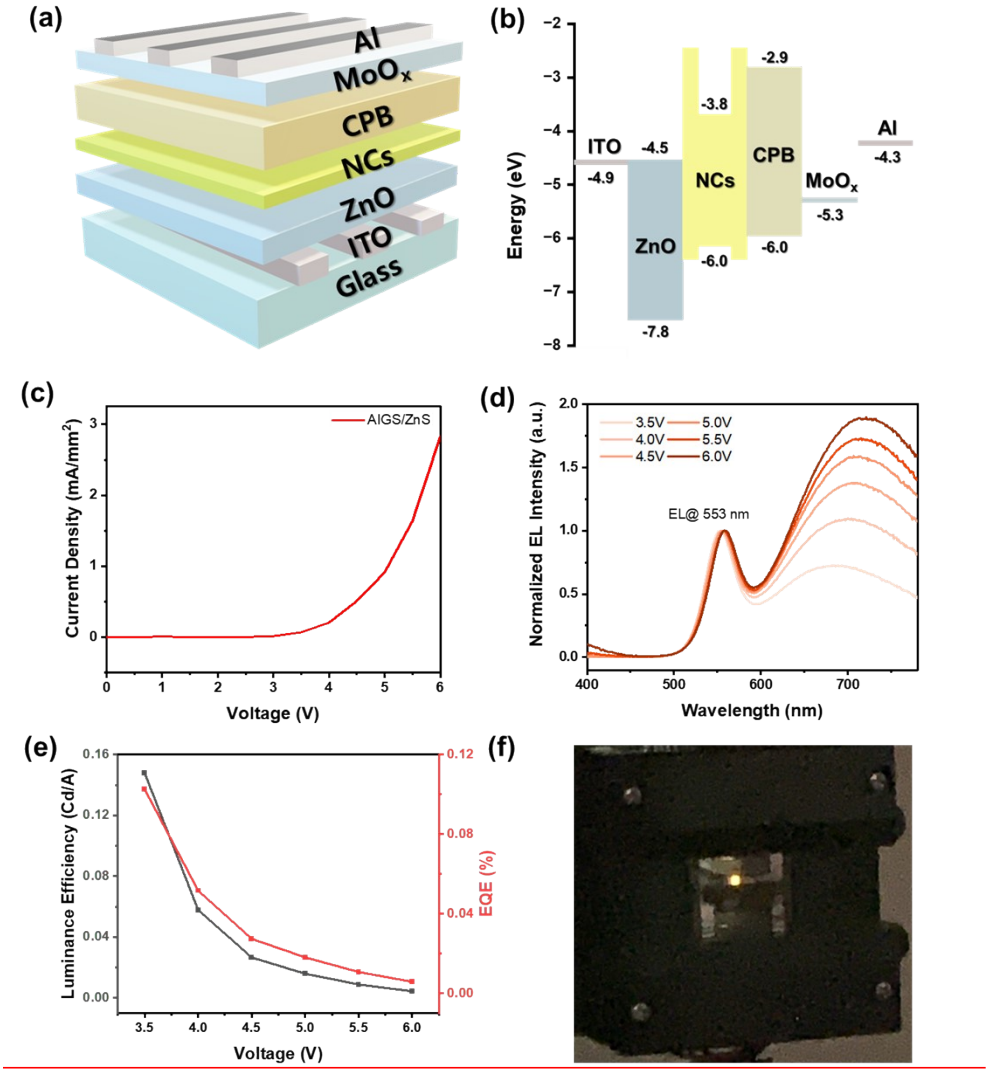

Figure S9. Absorption and PL spectrum of AIGS/ZnS NCs used in the EL device

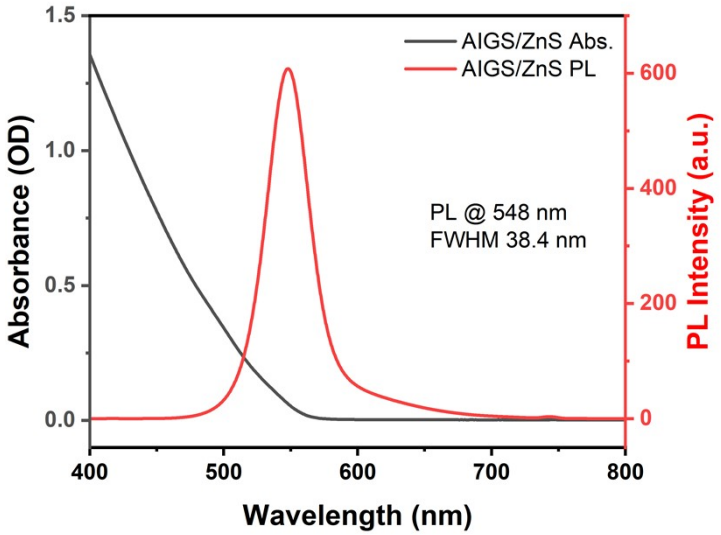

Figure S10. (a) E_{onset}, (b) E_{offset} of AIGS NCs fitted by ultraviolet photoelectron spectroscopy (UPS)

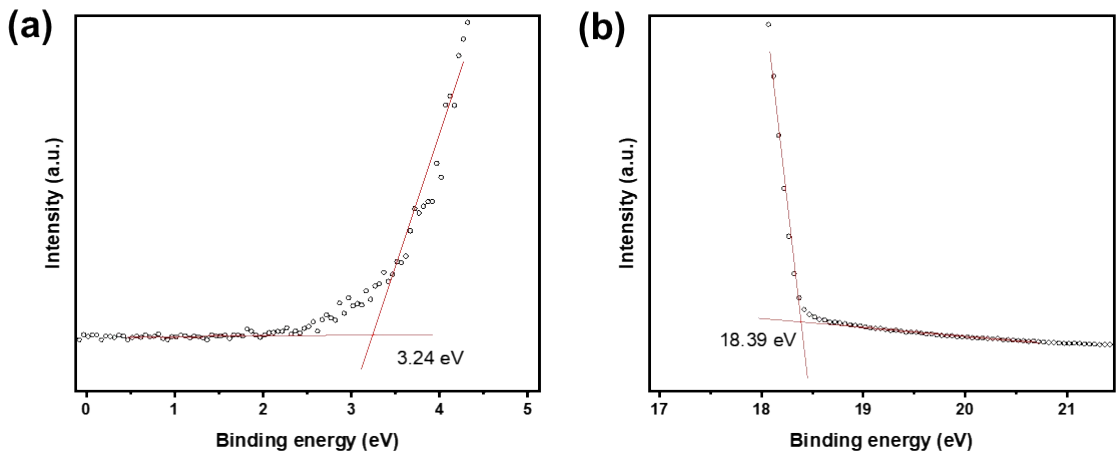

Reference

(1) Francesca Dalu, M. A. S., Claudio Cara, Alberto Luridiana, Anna Musinu, Mariano Casu, Francesco Secci, Carla Cannas. A catalyst-free, waste-less ethanol-based solvothermal synthesis of amides. *Green Chem* **2018**, *20*, 375-381. DOI: 10.1039/C7GC02967E.